MEMBRANES AND BIOENERGETICS:

Selective Cytotoxicity of Dermaseptin S3 toward IntraerythrocyticPlasmodium falciparum and the Underlying Molecular Basis

Jimut Kanti Ghosh, Dan Shaool, Philippe Guillaud, Liliane Cicéron, Dominique Mazier, Irina Kustanovich, Yechiel Shai and Amram Mor

J. Biol. Chem. 1997, 272:31609-31616.
doi: 10.1074/jbc.272.50.31609

THE JOURNAL OF BIOLOGICAL CHEMISTRY
Vol. 272, No. 50, Issue of December 12, pp. 31609–31616, 1997

Printed in U.S.A.

Selective Cytotoxicity of Dermaseptin S3 toward Intraerythrocytic *Plasmodium falciparum* and the Underlying Molecular Basis*

(Received for publication, July 28, 1997, and in revised form, September 8, 1997)

Jimut Kanti Ghosh‡§, Dan Shaool¶, Philippe Guillaud¶, Liliane Cicéron‖, Dominique Mazier‖, Irina Kustanovich, Yechiel Shai‡, and Amram Mor**‡‡**

*From the ‡Department of Membrane Research and Biophysics, The Weizmann Institute of Science, Rehovot 76100, Israel, ¶Service Imagerie, Institut Jacques Monod, 2 Place Jussieu, 75251 Paris Cedex 05, France, ‖INSERM U313, Faculté de Médecine Pitié-Salpêtrière, 75634 Paris Cedex 13, France, and **The Wolfson Center for Applied Structural Biology, The Hebrew University of Jerusalem, Givat Ram 91904, Jerusalem, Israel*

The antimicrobial activity of various naturally occurring microbicidal peptides was reported to result from their interaction with microbial membrane. In this study, we investigated the cytotoxicity of the hemolytic peptide dermaseptin S4 (DS4) and the nonhemolytic peptide dermaseptin S3 (DS3) toward human erythrocytes infected by the malaria parasite *Plasmodium falciparum*. Both DS4 and DS3 inhibited the parasite's ability to incorporate [^{3}H]hypoxanthine. However, while DS4 was toxic toward both the parasite and the host erythrocyte, DS3 was toxic only toward the intraerythrocytic parasite. To gain insight into the mechanism of this selective cytotoxicity, we labeled the peptides with fluorescent probes and investigated their organization in solution and in membranes. In *Plasmodium*-infected cells, rhodamine-labeled peptides interacted directly with the intracellular parasite, in contrast to noninfected cells, where the peptides remained bound to the erythrocyte plasma membrane. Binding experiments to phospholipid membranes revealed that DS3 and DS4 had similar binding characteristics. Membrane permeation studies indicated that the peptides were equally potent in permeating phosphatidylserine/phosphatidylcholine vesicles, whereas DS4 was more permeative with phosphatidylcholine vesicles. In aqueous solutions, DS4 was found to be in a higher aggregation state. Nevertheless, both DS3 and DS4 spontaneously dissociated to monomers upon interaction with vesicles, albeit with different kinetics. In light of these results, we propose a mechanism by which dermaseptins permeate cells and affect intraerythrocytic parasites.

Antimicrobial peptides are produced by prokaryotic and eukaryotic cells (1, 2). These natural antibiotics have been the subject of many studies in recent years due to their involvement in host defense mechanisms and for their potential use in therapeutics. They are now believed to be an essential defense component of invertebrates and vertebrates, including humans, destined to control cell proliferation and invading pathogens. Although the precise mechanism of action of antimicrobial peptides is not fully understood, most of such peptides known to date are believed to permeate the target cell by destabilizing its plasma membrane via either a "barrel stave" mechanism (3–5) or a nonpore carpet-like mechanism (6–8). These studies showed that despite a large heterogeneity in primary and secondary structures, antimicrobial peptides are active against a large spectrum of microorganisms, yet most of them are generally nontoxic toward mammalian cells. The molecular basis for this selectivity is still ill defined.

Dermaseptins are a family of structurally and functionally related peptides, isolated from the skin of tree frogs belonging to the *Phyllomedusa* genus (9–11). They are linear polycationic peptides, composed of 28–34 amino acids that are structured in amphipathic α-helix in apolar solvents (12). Accumulated data, using phospholipid liposomes (13, 14) or live cells (6) suggested that the antimicrobial action of these peptides is mediated by interaction of the amphipathic α-helix with the plasma membrane phospholipids. All dermaseptin peptides were shown to have a cytolytic activity *in vitro* against various pathogenic microorganisms (bacteria, protozoa, yeast, and filamentous fungi). Combination of five members (S1, S2, S3, S4, and S5) resulted in some cases in a 100-fold increase in the antibiotic activity over the activity of the peptides separately (15). The aim of the present study is to investigate the molecular basis for the selective cytotoxicity of different dermaseptins. For this purpose, we compared the interactions of the hemolytic peptide dermaseptin S4 (DS4)[1] and the nonhemolytic peptide dermaseptin S3 (DS3) with infected erythrocytes and with model phospholipid membranes. The peptides were labeled selectively at their N-terminal amino acids with 7-nitrobenz-2-oxa-1,3-diazole-4-yl (NBD) to facilitate binding experiments and to serve as an energy transfer donor or with rhodamine to serve as energy transfer acceptor. The selective cell permeation properties of DS3 and DS4 are discussed with respect to their organization in solution and after binding to membranes.

MATERIALS AND METHODS

Reagents—Fmoc-amino acids were from Milligen. HMP-linked polyamide/Kieselguhr resin and Fmoc-amino acid pentafluorophenyl and 3-hydroxy-2,3-dehydro-4-oxobenzotriazine esters were from Milligen/

* This research was supported by the Basic Research Foundation administrated by the Israel Academy of Sciences and Humanities (to Y. S.); by the DA'AT consortium, a Magnet project administrated by the Office of the Chief Scientist at the ministry of Industry and Trade, Israel; and by l'Agence Nationale pour la Recherche contre le SIDA (ANRS), France. The costs of publication of this article were defrayed in part by the payment of page charges. This article must therefore be hereby marked "*advertisement*" in accordance with 18 U.S.C. Section 1734 solely to indicate this fact.

§ Recipient of a Sir Charles Clore postdoctoral fellowship from the Feinberg Graduate School, the Weizmann Institute of Science, Israel.

‡‡ To whom correspondence should be addressed: The Wolfson Center for Applied Structural Biology, The Hebrew University of Jerusalem, Givat Ram 91904, Jerusalem, Israel. Tel.: 972-2-65-85-578; Fax: 972-2-65-85-573; E-mail: amor@macbeth.ls.huji.ac.il.

[1] The abbreviations used are: DS4, dermaseptin S4; DS3, dermaseptin 3; Fmoc, *N*-(9-fluorenyl)methoxycarbonyl; NBD, 7-nitrobenz-2-oxa-1,3-diazole-4-yl; PC, phosphatidylcholine; PS, phosphatidylserine; diS-C2–5, diethylthiodicarbocyanine iodide; HPLC, high pressure liquid chromatography; SUV, small unilamellar vesicles; RBC, red blood cells; PBS, phosphate-buffered saline; DIC, differential interference contrast mode.

Bioresearch. Other reagents for peptide synthesis were obtained from Sigma. Calcein was purchased from Hach Chemical Co. (Loveland, CO). L-α-Phosphatidylcholine (type IVS) was obtained from Sigma. Egg phosphatidylcholine (PC) and phosphatidylserine (PS) from bovine spinal cord (sodium salt, grade I), were purchased from Lipid Products (South Nutfield, United Kingdom). Diethylthiodicarbocyanine iodide (diS-C2–5), NBD-F(4-fluoro-7-nitrobenz-2-oxa-1,3-diazole), and tetramethyl rhodamine were obtained from Molecular Probes (Eugene, OR). All other reagents were of analytical grade. Buffers were prepared using double glass-distilled water.

Peptide Synthesis, Fluorescent Labeling, and Purification—The peptides were synthesized by a solid phase method, applying the Fmoc active ester chemistry on a Milligen 9050 Pepsynthesizer. After removal of the Fmoc from the N-terminal amino acid, the peptide was cleaved from the resin with a mixture of 85:5:5:5 trifluoroacetic acid:*p*-cresol:H_2O:thioanisole (10 mg of resin-bound peptide in a 1-ml mixture). The trifluoroacetic acid was then evaporated, and the peptide was precipitated with ether followed by washing with ether (4 times). The crude peptide was extracted from the resin with 40% acetonitrile in water and was purified to chromatographic homogeneity in the range of 95 to >99% by reverse phase HPLC on a semipreparative C18 column using a linear gradient of 30–80% acetonitrile in water (both containing 0.1% trifluoroacetic acid) in 40 min. The purified peptide was subjected to amino acid analysis and fast atom bombardment mass spectrometry to confirm its composition.

Labeling of the peptide at its N-terminal amino acid with fluorescent probes was performed on resin-bound peptide as described previously (16). Briefly, 20–30 mg of resin-bound peptide (~6 mmol) were treated with piperidine in dry dimethylformamide to remove the Fmoc protecting group of the N-terminal amino acid of the linked peptide. The resin-bound peptide was then reacted with (i) 4-fluoro-7-nitrobenz-2-oxa-1,3-diazole in dry dimethylformamide or (ii) tetramethylrhodamine succinimidyl ester (3–4 eq) in dry dimethylformamide containing 5% (v/v) diisopropylethylamine. After 24 h, the resin-bound peptides were washed thoroughly with methylene chloride, and then the peptides were cleaved from the corresponding resins, precipitated with ether, extracted, and purified as described above. Peptides were kept as lyophilized powder at −80 °C. Prior to being tested, fresh solutions were prepared in water, vortexed, sonicated, centrifuged, and then diluted in the required medium.

NMR Samples and Measurements—Samples for one-dimensional NMR experiments were prepared by dissolving 2 mg of lyophilized S3 or S4 in 0.5 ml containing 90% H_2O and 10% D_2O. NMR experiments were carried out at 600.13 MHz on a Bruker DMX-600 AVANCE spectrometer at room temperature. The carrier frequency was set on the water resonance signal, and it was presaturated during the relaxation delay of 1.5 s. For both samples, 16,384 data points were collected, with a spectral width of 8 kHz. Data processing was performed using Bruker's XWINNMR software, and all spectra were calibrated *versus* tetramethylsilane.

Preparation of Liposomes—Small unilamellar vesicles (SUV) were prepared by sonication of PC or PC/PS (1:1, w/w) as described previously (17, 18). The lipid concentrations of the resulting preparations were determined by phosphorous analysis (19). Transmission electron microscopy (JEOL JEM 100B electron microscope, Japan Electron Optics Laboratory Co., Tokyo, Japan) was used to visualize the morphology of the vesicles as follows. A drop of vesicles was deposited on a carbon-coated grid and negatively stained with uranyl acetate. Examination of the grids demonstrated that the vesicles were unilamellar with an average diameter of 20–50 nm (20).

NBD Fluorescence Measurements and Binding Experiments—NBD-labeled peptides (0.2 μM) were added to 2 ml of PBS buffer (150 mM NaCl, 10 mM sodium phosphate, pH 7.3) containing PC or PS/PC SUV (360 μM), to establish a lipid/peptide ratio (1:1800) in which most of the peptide will be bound to lipids. After a 15-min incubation, the emission spectrum of NBD-labeled peptide in the presence of lipid vesicles (either PC or PS/PC) was recorded (in three separate experiments) using a Perkin-Elmer LS-50B spectrofluorimeter, with the excitation wavelength set at 467 nm (10-nm slit). Binding determinations were performed as described previously (15). Briefly, PC or PS/PC SUVs were added gradually to 0.2 μM of NBD-labeled dermaseptins at room temperature. Fluorescence intensities were measured as a function of the lipid/peptide molar ratios on a Perkin-Elmer LS-50B Spectrofluorimeter, with the excitation set at 467 nm, using a 10-nm slit, and the emission was set at 530 nm, using a 5-nm slit, in three separate experiments. The extent of the lipids' contribution to any given signal was determined using readings obtained when unlabeled peptides were titrated with lipid vesicles and was subtracted as background from the recorded fluorescence intensities.

Resonance Energy Transfer Measurements—Fluorescence spectra were obtained at room temperature in a Perkin-Elmer LS-50B spectrofluorimeter, with the excitation monochromator set at 467 nm (to minimize the excitation of tetramethylrhodamine) and with a 5-nm slit width. Measurements were performed in a 1-cm path length glass cuvette and a final reaction volume of 2 ml. In a typical experiment, donor (NBD-labeled) peptide at a final concentration of 0.2 μM was added to a dispersion of PC or PS/PC SUV (360 μM) in PBS buffer, followed by addition of the acceptor (Rho-labeled) peptide in several sequential doses. Fluorescence spectra were obtained before and after the addition of the acceptor peptide. Changes in the fluorescence intensity of the donor (due to processes other than energy transfer to the acceptor) were determined by substituting unlabeled peptide for the acceptor and by measuring the emission spectrum of the acceptor alone in the presence of vesicles.

The efficiency of energy transfer (E) was determined by measuring the decrease in the quantum yield of the donor as a result of the addition of acceptor. E was determined experimentally from the ratio of the fluorescence intensities of the donor in the presence (Ida) and in the absence (Id) of the acceptor at the donor's emission wavelength, after correcting for membrane light scattering and the contribution of acceptor emission. The correction for light scattering was made by subtracting the signal obtained when unlabeled analogues were added to vesicles containing the donor molecule. Correction for the contribution of acceptor emission was made by subtracting the signal produced by the acceptor-labeled analogue alone. The percentage of transfer efficiency (E) is defined as follows: $E = (1 - Ida/Id) \times 100$.

Membrane Permeability Assay—Membrane destabilization, which results in the collapse of diffusion potential, was detected fluorimetrically, as described previously (21, 22). A liposome suspension, prepared in "K^+ buffer" (50 mM K_2SO_4/25 mM HEPES-sulfate, pH 6.8), was added to an isotonic K^+-free buffer (50 mM Na_2SO_4/25 mM of HEPES-sulfate, pH 6.8), and the dye diS-C2–5 was then added. The subsequent addition of valinomycin created a negative diffusion potential inside the vesicles by a selective efflux of K^+ ions, which resulted in a quenching of the dye's fluorescence. Peptide-induced membrane permeability for all of the ions in the solution caused a dissipation of the diffusion potential, as monitored by an increase in fluorescence. Fluorescence was monitored using excitation and emission wavelengths at 620 and 670 nm, respectively. The percentage of fluorescence recovery (Ft) was defined as $Ft = ((It - Io)/(If - Io)) \times 100\%$, where It represents fluorescence observed after the addition of a peptide at time t, Io is fluorescence after the addition of valinomycin, and If is total fluorescence prior to the addition of valinomycin.

Erythrocytes—Fresh heparinized human blood was rinsed three times in PBS (50 mM sodium phosphate, 150 mM NaCl, pH 7.3) by centrifugation for 5 min at 900 × g; alternatively, whole blood was used. For the hemoglobin release assay, 2×10^8 RBC/ml were treated at room temperature in Eppendorf tubes by adding a 50-μl cell suspension to 200 μl of PBS containing various peptide concentrations. Treated suspensions were either analyzed immediately or incubated for various periods of time. Hemolytic activity was assessed as a function of hemoglobin leakage in the suspension as monitored by measuring the absorbance of the supernatant at 541 nm after centrifugation at 900 × g. Control cells were treated with distilled water or with PBS for 100% hemolysis and base-line values, respectively. The percentage of hemolysis was calculated taking into account the absorbance measured again for each sample after lysis with distilled water.

Peptide Binding to Erythrocytes—For cell binding experiments, a 50-μl suspension containing 1×10^7 RBC were added at room temperature to 200 μl of PBS containing various peptide concentrations in Eppendorf tubes. After brief vortexing and centrifugation, the supernatant was analyzed by HPLC as detailed above. The amount of peptide present in the supernatant (free peptide) was calculated using standard curves of known concentrations for each peptide. To investigate the reversibility of the peptides binding, the pellets were washed (3 times) in PBS and then incubated in 250 μl of PBS under various conditions of time and temperature, including in the presence of fresh 1×10^7 RBC.

Antiparasite Activity of DS3 and DS4—The cytotoxicity toward *Plasmodium falciparum* in its erythrocytic stage was evaluated using the microtest method of Desjardin (23), which is based on the measure of incorporated radiolabeled hypoxanthine by the parasite in presence of increasing drug concentrations. The method was modified as follows. The infection rate prior to the drug addition was 0.5% (determined by counting an aliquot on RAL-stained smears), and the parasites' exposure to hypoxanthine was 48 h. The parasites tested were isolated from patients who contracted the palludism in Nigeria and adapted to con-

TABLE I
Primary structure of the dermaseptin peptides and their fluorescently labeled analogs

Designation	Amino acid sequence
DS3 (X = H) NBD-DS3 (X = NBD) Rho-DS3 (X = rhodamine)	*X*-ALWKNMLKGIGKLAGKAALGAVKKLVGAES
DS4 (X = H) NBD-DS4 (X = NBD) Rho-DS4 (X = rhodamine)	*X*-ALWMTLLKKVLKAAAKAALNAVLVGANA

tinuous culture as described (24). Three parasite strains were tested; two strains (H and NF54) are characteristically sensitive to chloroquine (25), and the third is a chloroquine-resistant strain (Ibrahim). The assay was performed in sterilized 96-well microtiter plates (Nunc F96, Denmark). Serial 2-fold dilutions of chloroquine or peptide (34.0–0.06 μM) were performed in complete culture medium (RPMI 1640, 35 mM HEPES, 2 g/liter glucose, 2.1 g/liter sodium bicarbonate, 10 mg/liter gentamicine, and 10% decomplemented AB serum). To the 50-μl drug dilutions, 200 μl of culture medium containing 9 μl of parasite suspension (50% hematocrite) and 1.6 μCi of [^{3}H]hypoxanthine (Amersham, France) were added. For positive growth controls, cells were cultured in drug-free medium. After a 48-h incubation at 37 °C, the content from each well was transferred to a paper filter using a cell collector (Skatron Instruments, Norway). Radioactivity was counted in scintillation liquid (Beckman LS 1701).

Videomicroscopy—Visual information on peptide interactions with RBC was obtained using a computer-assisted image analysis system (Oncor, UK), coupled to a cooled low level CCD camera (Photometrics) and an epiillumination inverted Axiovert microscope (Zeiss). Red fluorescence images were acquired with a band pass filter BP 546/12 nm, a chromatic beam splitter FT580, and a long wave pass filter LP 590 nm. An adaptable cell culture chamber was used to realize experiments. Cells (2×10^8 RBC/ml in PBS) deposited in the culture chamber 5 min prior to the peptide addition were allowed to settle at the bottom and form a carpet, and then the peptide was added in a drop at the center. Images were acquired with a plan-apochromat 100/1.4 oil immersion objective (Zeiss). Transmitted light images were realized in differential interference contrast mode (DIC). Images were digitized in a 512×512 array, and fluorescence or transmission intensity levels were primary coded on 16 bits. Images were then exported in 8 bits TIFF format. NIH Image 1.61 (by Wayne Rasband, NIH) and Photoshop 3.0 (Adobe) programs were used to make the printed outputs on a Kodak Colorease sublimation laser printer.

RESULTS

Toward understanding the molecular mechanisms involved in the selective cytotoxicity of dermaseptins, various labeled and unlabeled versions of DS3 and DS4 (the peptides and their designations are listed in Table I) were investigated at three different levels: peptide interaction with target cells (erythrocytes and intraerythrocytic parasites), peptide-peptide interaction in solution, and peptide interaction with model phospholipid membranes (the hypothetical primary target).

Interaction of DS3 and DS4 with Target Cells

Interaction of DS4 with Erythrocytes—Incubation of washed erythrocytes (without serum) for 1 h in the presence of DS4 resulted in hemoglobin release corresponding to 50% cell lysis at the peptide concentration of 0.5 μM and 100% lysis at 1 μM (Fig. 1*A*). Ten-fold higher concentrations were needed to induce the same effect (not shown) when unwashed blood (with serum) was used, indicating that a significant amount of the peptide was captured by serum components.

Further information on the nature of the interaction of DS4 with erythrocytes was obtained from microscopical studies. In experiments using a microscope linked to a video camera, cells were allowed to settle at the bottom of the reaction chamber before the peptide was added. The addition of the peptide (labeled or unlabeled) resulted in instantaneous hemolysis; *i.e.* within 5 s from peptide addition, the voluminous round cells collapsed and turned into flat ghosts. The ghosts were labeled exclusively at their periphery, where peptide aggregates were clearly observable (Fig. 1*B*).

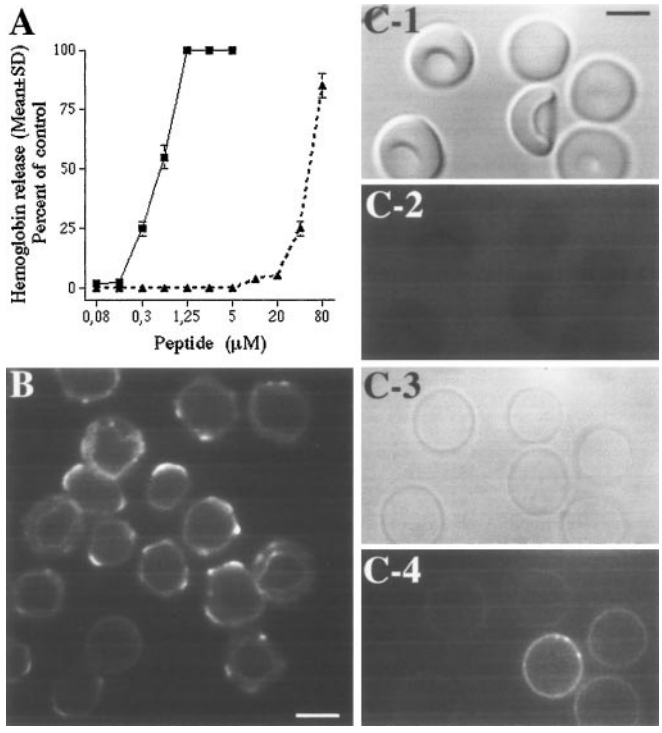

FIG. 1. **Interaction of DS3 and DS4 with erythrocytes.** *A*, hemolytic activity of DS3 (*triangles*) and DS4 (*rectangles*) following a 1-h incubation with rinsed human red blood cells (2.5×10^8/ml) in PBS. Control cells were treated with distilled water or with PBS for 100% hemolysis and base-line values, respectively. *B*, fluorescence videomicroscopy image of erythrocytes approximately 5 s after the addition of Rho-DS4 (1 μM). *Bar*, 5 μm. *C*, visualization by videomicroscopy of Rho-DS3-treated erythrocytes. The addition of Rho-DS3 (1 μM) did not lyse the cells (*C-1*, DIC image; *C-2*, fluorescence image); the addition of water induced ghost formation (*C-3*, DIC image) which unraveled labeling of the plasma membrane (*C-4*, fluorescence image). *Bar*, 5 μm.

HPLC analysis of the posthemolysis supernatant indicated that DS4 binding to RBC was of a linear nature over a wide range of concentrations (Fig. 2), since only traces of free peptide could be detected at 250 μg/ml (not shown). To investigate the reversibility of the binding, the pellets were washed and reincubated in 250 μl of PBS and then analyzed in HPLC. No trace of free peptide could be detected after overnight incubation at 37 °C, indicating that DS4 remains cell-bound and does not diffuse out back to the aqueous solution. Interestingly, incubation of the washed pellets (pretreated with 10 μM DS4) in the presence of fresh RBC induced instant hemolysis, and full hemolytic activity was recovered within 1 h of incubation (not shown). Moreover, such secondary hemolysis was observed after several repeats of the following cycle: hemolysis, wash, and the addition of fresh RBC.

Interaction of DS3 with Erythrocytes—Fig. 1*A* shows that DS3 also induced hemolysis of washed erythrocytes. However, the DS3-induced hemolysis was 100-fold less efficient than DS4

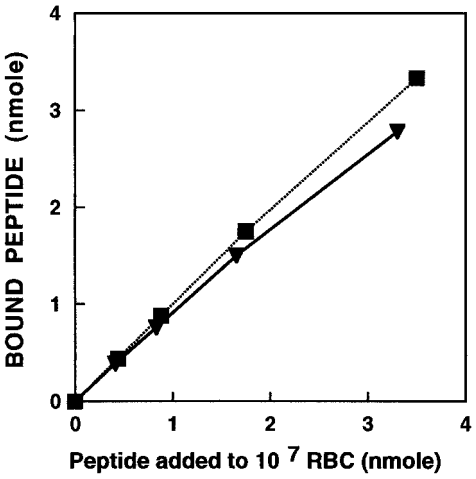

FIG. 2. **Binding of DS3 (*triangles*) or DS4 (*rectangles*) to red blood cells.** 1×10^7 RBC (50 μl) were added to 200 μl of PBS containing various peptide concentrations, and the supernatants were analyzed by reversed-phase HPLC. The peptide present in the supernatant (free peptide) was calculated using standard curves of known concentrations for each peptide.

(50% hemolysis at 50 μM). Evidence for the peptide interaction with erythrocytes at nonhemolytic concentration was obtained from HPLC analysis of the supernatant after treatment with DS3 under the same conditions as for DS4. Fig. 2 shows that DS3 bound to RBC almost to the same extent as DS4 yet did not induce massive hemolysis (2.6% hemoglobin released at 10 μM). There was no evidence for peptide degradation products.

Confirmation for peptide binding to the red cells was obtained from visualization of Rho-DS3-treated RBC (Fig. 1*C*). Observation under a fluorescence microscope revealed that intact cells were not labeled. This suggested that only those cells that bound the peptide were permeabilized. However, lysis of the cells upon water addition, revealed that in reality, most if not all cells interacted with Rho-DS3, but the bound peptide could not be visualized in hemoglobin-containing cells, most probably because the fluorescence emitted by rhodamine at 541 nm is absorbed by hemoglobin. Once the hemoglobin was released, the fluorescence became immediately visible. Taken together, these experiments indicated that although DS3 binds to erythrocytes, cell permeabilization occurs only when a critical concentration is achieved, in contradiction to DS4, where low peptide concentrations induced massive hemolysis.

Interaction of DS3 and DS4 with Infected Erythrocytes—To investigate the interaction of the dermaseptins with cells whose plasma membrane is not "*a priori*" accessible, we investigated the peptides interaction with *P. falciparum* in its erythrocytic stage. Within seconds after the addition of Rho-DS3 (10 μM), fluorescence videomicroscopy analysis indicated that in infected cells the peptides accumulated within the parasite, and the erythrocyte plasma membrane was generally only faintly labeled or not labeled at all (Fig. 3). Rapid accumulation within the parasite was also observed with Rho-DS4 (10 μM) (Fig. 3, *a* and *b*). This sharply contrasted with the labeling patterns of noninfected cells, where DS3 and DS4 labeled the erythrocytes plasma membrane only (Fig. 1, *panels B* and *C-4*).

Antiparasite Activity of DS3 and DS4—To investigate the fate of the interaction between the antimicrobial peptides and the intraerythrocytic parasite, we assessed the viability of the parasite by measuring the [^{3}H]hypoxanthine incorporated after 48 h of culture. Both DS3 and DS4 affected the viability of the malaria parasite, since hypoxanthine incorporation was inhibited in a dose-dependent manner (Fig. 4) using either the chloroquine-sensitive strains, strain H (IC_{50} 0.8 and 2.2 μM, respectively) and strain NF54 (IC_{50} 0.26 and 0.27 μM, respectively), or the chloroquine-resistant strain Ibrahim (IC_{50} 1.5 and 2.0 μM, respectively). In these cultures, DS3 was cytotoxic only for the malaria parasite, since no hemolysis could be detected up to 34.0 μM, whereas DS4 became toxic also for erythrocytes at high peptide concentrations (hemolysis was observed at concentrations higher than 8.5 μM).

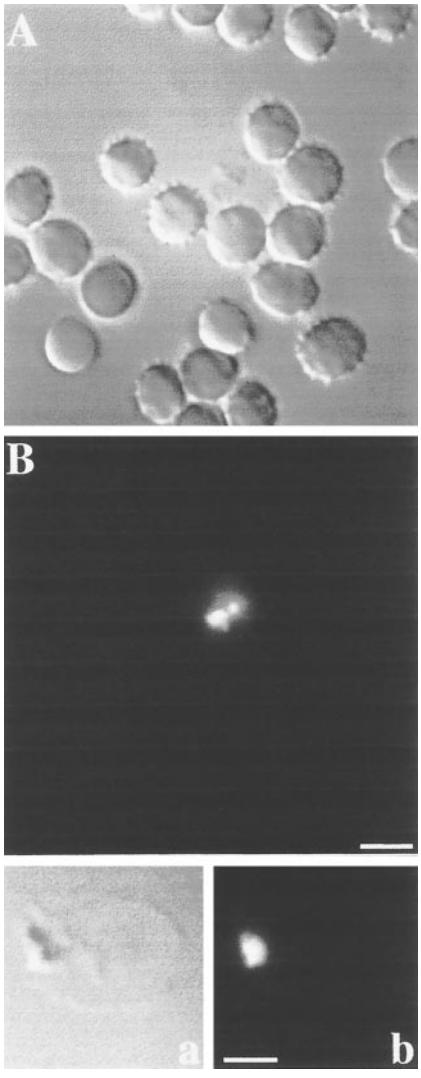

FIG. 3. **Videomicroscopy images of *Plasmodium*-infected erythrocytes (infection rate 0.5%).** Images were taken approximately 5 s after the peptide addition. *A*, DIC image, showing that most cells remain intact after the addition of Rho-DS3 (10 μM). *B*, fluorescence image, showing a ghost cell that is infected and labeled. *Bar*, 10 μm. *Lower panels*, DIC (*a*) and fluorescence (*b*) zoom images obtained after the addition of Rho-DS4 (1 μM) as described for *panels A* and *B*. *Bar*, 2 μm.

Organization of DS3 and DS4 in Solution

Fluorescence Studies—The aggregational properties of DS3 and DS4 in aqueous solution were determined using rhodamine-labeled peptides. This detection is based on the self-quenching of rhodamine fluorescence when several rhodamine labeled peptides are in close proximity, *i.e.* in an aggregated state. An increase in fluorescence should occur when the aggregated rhodamine-labeled peptide is dissociated, a process that should take place when the peptide is cleaved by proteolytic enzymes. The results summarized in Fig. 5 indicate these properties. The *black columns* represent the fluorescence of Rho-DS3 (0.520 μM) and Rho-DS4 (0.529 μM) in solution. Al-

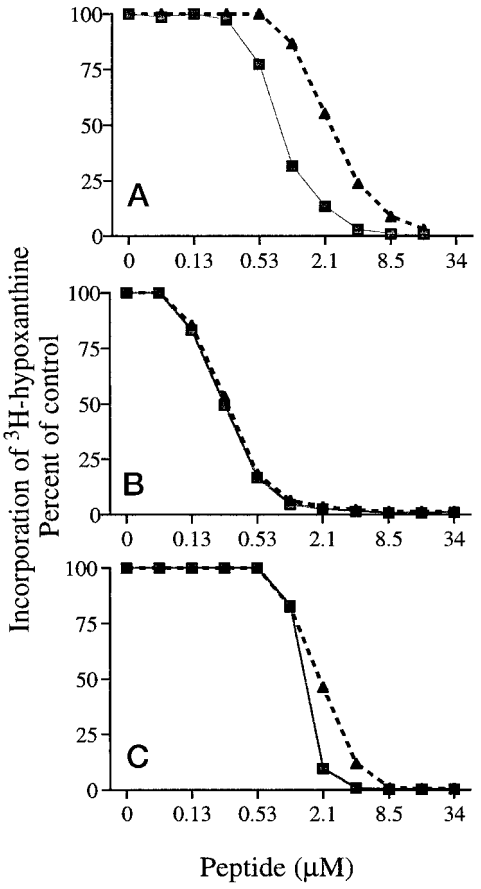

FIG. 4. **Inhibition of incorporation of [^{3}H]hypoxanthine by *P. falciparum*-infected erythrocytes after a 48-h incubation in the presence of DS3 (*triangles*) or DS4 (*rectangles*).** *A*, chloroquine-sensitive strain H; *B*, chloroquine-sensitive strain NF54; *C*, chloroquine-resistant strain Ibrahim. Mean incorporation value of control (drug-free) cells was 11 ± 1 × 10^3 cpm. Plotted values represent the mean of duplicated experiments. Variations were within 10%.

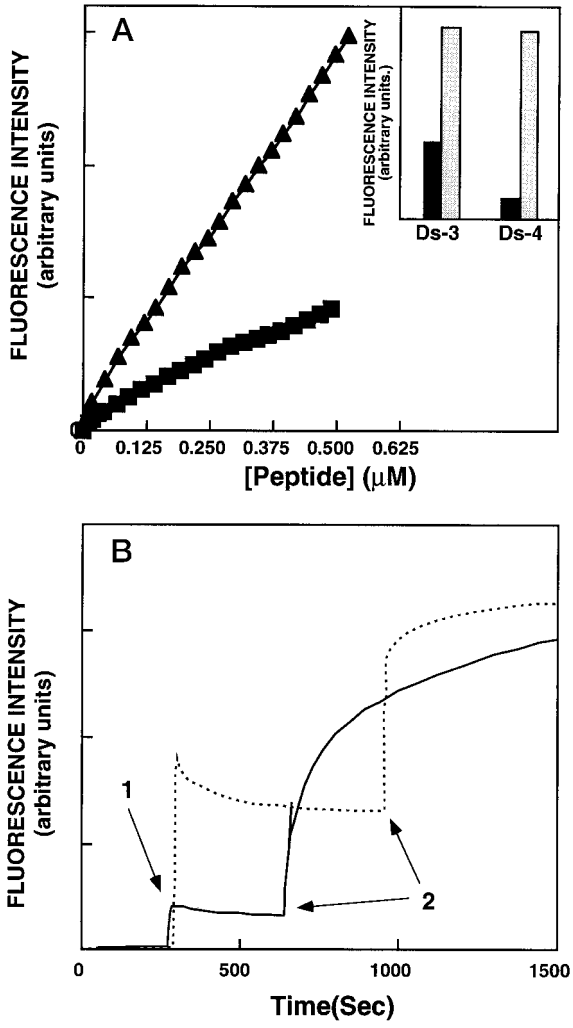

FIG. 5. **Aggregation of DS3 and DS4 in solution and their dissociation in membranes.** In *panel A*, the aggregation states of Rho-DS3 (*triangles*) and Rho-DS4 (*squares*) are detected by plotting the concentration dependence fluorescence of the peptides in PBS. Excitation was set at 530 nm and emission at 575 nm. *Inset*, initial fluorescence of 0.52 μM of either Rho-DS3 or Rho-DS4 (*filled columns*) and final fluorescence upon the addition of proteinase K (*empty columns*). *Panel B* shows the increase in the fluorescence of 0.5 μM of either Rho-DS3 (*dotted line*) or Rho-DS4 (*solid line*) upon the addition of 360 μM PS/PC vesicles in PBS. Excitation and emission were as above. Time points indicate the addition of peptides (1) and liposomes (2).

though the concentrations of Rho-DS3 and Rho-DS4 were nearly equal, Rho-DS4 was less fluorescent (<50%), indicating its higher aggregation state. The addition of proteinase K caused dequenching of fluorescence to Rho-DS3 and Rho-DS4, indicating that proteolysis disrupts the aggregation state. Expectedly, when the peptides were cleaved by proteinase K they exhibited very similar levels of fluorescence. Moreover, to understand the nature of the aggregation state, the dose-dependent fluorescence values of the peptides were recorded at 575 nm (characteristic of rhodamine emission peak). *Panel A* of Fig. 5 depicts two such plots of fluorescence *versus* concentration of Rho-DS3 and Rho-DS4. The linear nature of the Rho-DS3 plot suggests that Rho-DS3 does not change its state beyond 0.1 μM, whereas the plot for Rho-DS4 deviates from linearity around 0.1 μM, indicating its change in aggregational state at this concentration range. Combining both results, it can be concluded that (i) both DS3 and DS4 are aggregated in aqueous solutions; (ii) the aggregational state of DS4 is higher than that of DS3; and (iii) once DS3 forms an aggregate at very low concentration, it does not change its aggregational state, whereas DS4 changes its aggregational state with increasing concentrations.

NMR Studies—One-dimensional proton NMR analysis of the peptides provided further support to the conclusions drawn from the fluorescence studies concerning the higher aggregation state of DS4. The recorded NMR spectra (not shown) presented the amide and the aromatic regions of the spectrum. Straightforward comparison of the two traces immediately revealed a difference in their spectral appearances: the spectrum of DS3 exhibited sharp well resolved resonances, while the spectrum obtained for DS4 consisted of several broad overlapped lines lacking fine multiplet structures (26). These observations strongly suggested that the two peptides experience different molecular organizations in water solution. The poor resolution of the DS4 spectrum is typical of peptides with higher molecular weight, indicating that DS4 molecules undergo an association process and are present as aggregates. The mobility of DS4 molecules within those assemblies is highly reduced, and they can undergo restricted motions characterized by slow (on an NMR time scale) correlation times. On the other hand, DS3 gave rise to the high resolution spectrum characteristic to the monomers rotating freely in solution.

Interaction of DS3 and DS4 with Model Membranes

Localization of the Environment of the NBD Moiety—Due to the sensitivity of the fluorescence of NBD to the polarity of its environment, it has been used for polarity and binding studies

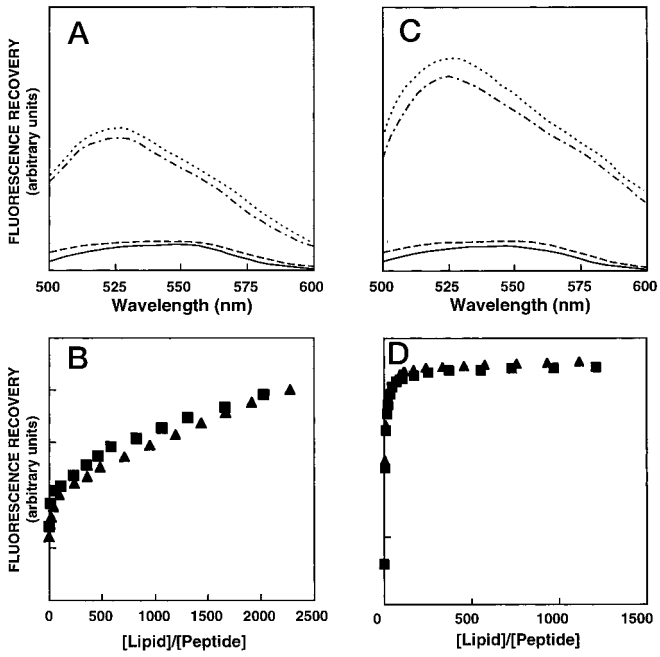

FIG. 6. **The effect of liposomes on the fluorescence of DS3 and DS4.** *A*, fluorescence emission spectra of 0.2 μM NBD-labeled peptides in solution and in the presence of 360 μM PC SUV (excitation 467 nm). Shown are NBD-DS3 before (*dashed line*) and after (*dashed dotted line*) the addition of vesicles and NBD-DS4 before (*continuous line*) and after (*dotted line*) the addition of vesicles (1:1). *B*, increase in the fluorescence of NBD-DS3 (*triangles*) and NBD-DS4 (*squares*) upon titration with PC vesicles. NBD-labeled peptides (0.2 μM) in buffer were titrated with SUV (excitation 470 nm, emission 530 nm). *C*, fluorescence emission spectra of 0.2 μM NBD-peptides in PBS buffer and in the presence of 360 μM PS/PC (1:1) SUV (excitation 467 nm). *D*, increase in the fluorescence of NBD-peptides upon titration with PS/PC vesicles. *Symbols* and *lines* in *C* and *D* are as for *A* and *B*, respectively.

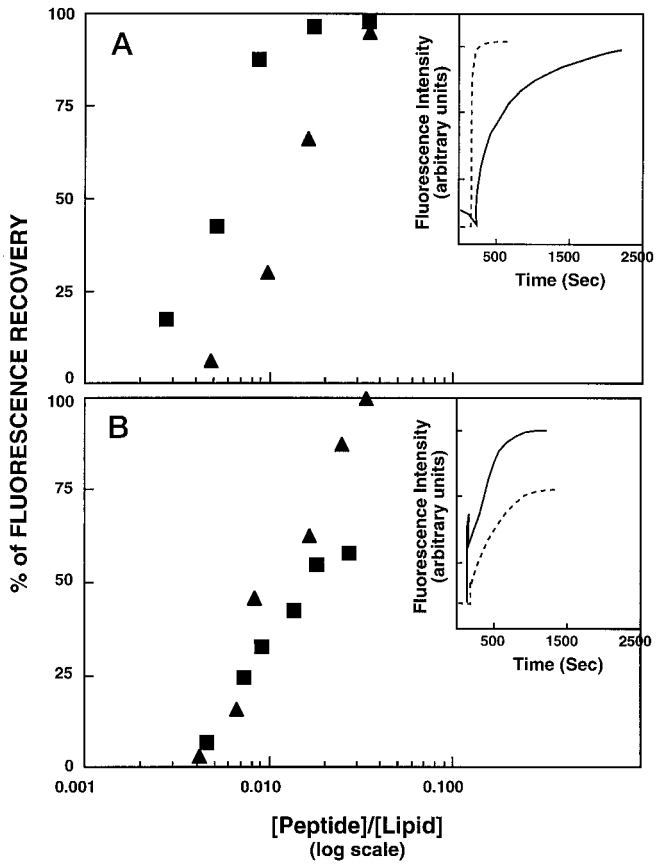

FIG. 7. **Dissipation of the diffusion potential in vesicles induced by DS3 and DS4.** The peptides were added to isotonic K^+-free buffer containing SUV composed of PC (*A*) or PC/PS (*B*) preequilibrated with the fluorescent dye diS-C2–5 and valinomycin. Fluorescence recovery was measured 10–30 min after the peptides were mixed with the vesicles. *Squares*, DS4; *triangles*, DS3. *Inset*, kinetics of fluorescence recovery after the addition of DS3 (*continuous line*) and DS4 (*broken line*) to PC (*A*) or PS/PC (*B*) at a peptide/lipid ratio of 0.035.

(27–30). To monitor the environment of the N termini of DS3 and DS4, the peptides were labeled at their N-terminal amino acid by the fluorescent probe NBD. Fluorescence emission spectra of the NBD-labeled peptides were monitored in PBS and in the presence of vesicles composed of either PC or PC/PS at pH 7.2. In these fluorometric studies, SUVs were used to minimize differential light scattering effects (31), and the lipid/peptide molar ratio was maintained high (1800:1) so that the spectral contributions of free peptide would be negligible. In buffer, both NBD-DS3 and NBD-DS4 exhibited a maximum of fluorescence emission at 545 nm, which reflects a hydrophilic environment for the NBD moiety (32). However, when vesicles were added to the aqueous solutions containing NBD-labeled peptides, blue shifts in the emission maxima (toward 525 ± 1 nm) and an increase in the fluorescence intensity of the NBD moieties were observed for both peptides in the presence of PC (Fig. 6*A*) and PS/PC (Fig. 6*C*) vesicles. The change in the spectrum of the NBD moiety reflects its relocation to a more hydrophobic environment (33). This blue shift is similar to that observed for an NBD group located within the membrane (32, 33) and is lower than those obtained for the nonhemolytic antibacterial peptides dermaseptins S1 and B1 (6, 14) or cecropins B and P (34, 35). The location of the peptides inside the membrane was further demonstrated by stability of the peptides to enzymatic degradation in their membrane-integrated state. No change in NBD fluorescence was observed following the treatment by proteinase K, due to their location inside the lipid vesicles in either PC or PS/PC (data not shown).

Membrane Partitioning—The affinity of DS3 and DS4 for phospholipid membranes was determined by titration of the NBD-labeled peptide (0.2 μM) with lipid vesicles in PBS buffer as described under "Materials and Methods." The fluorescence intensity was measured with excitation set at 467 nm and emission set at 530 nm. The fluorescence values were corrected by taking into account the dilution factor corresponding to the addition of microliter amounts of liposomes and by subtracting the corresponding blank (buffer with the same concentration of vesicles). To generate a binding curve, increasing fluorescence intensities of the NBD-labeled peptides upon the addition of vesicles were plotted as a function of the lipid/peptide molar ratios (Fig. 6, *B* and *D*, respectively, for PC and PS/PC). Since DS3 and DS4 are aggregated in solution, their corresponding binding isotherms were not analyzed. However, finding that the binding curves obtained for DS3 and DS4 are of a similar nature suggests that the peptides have similar affinity for either PC or PS/PC vesicles.

Membrane Permeabilization—Dermaseptins S3 and S4 and their fluorescent derivatives were examined for their efficacy in perturbing the lipid packing and causing leakage of vesicular contents by utilizing the dissipation of diffusion potential assay. Increasing peptide concentrations were mixed either with PC or with PS/PC SUV that had been pretreated with the fluorescent, potential-sensitive dye diS-C2–5 and valinomycin. Recovery of fluorescence was monitored as a function of time and usually occurred within 10–20 min. Maximal activity of dermaseptins was plotted *versus* peptide/lipid molar ratios. Fig. 7*A* depicts a plot of the percentage of fluorescence recovery induced by DS3 and DS4 in PC vesicles. It is evident from *panel A* that DS4 has higher efficacy compared with DS3 (particular-

ly at lower concentration) in disturbing the packing of the PC lipid bilayer. The recovery of the DS4-induced fluorescence is much faster than that of DS3 (*inset* of *panel A*). At a low peptide/lipid ratio, DS3 and DS4 exhibited similar activity in dissipation of diffusion potential in PS/PC vesicles, as reflected by the similar change of fluorescence recovery (Fig. 7*B*). Interestingly, it was found that DS3 and DS4 have very similar kinetics in inducing dissipation of diffusion potential (*inset* of *panel B*). The membrane-permeating activity of the fluorescently labeled dermaseptins was found identical to that obtained with the unlabeled peptides (data not shown).

Organization within the Membrane—To address the question of whether the peptides exist as monomers or oligomers within the lipid bilayer, the fluorescence of rhodamine-labeled peptides was monitored in the presence of phospholipid vesicles. Fig. 5*B* shows the changes in the fluorescence intensity of Rho-DS3 (*dotted line*) and Rho-DS4 (*solid line*) in the presence of vesicles. The addition of lipid vesicles caused an increase of fluorescence of both Rho-DS3 and Rho-DS4 in aqueous solution. Since the fluorescence of rhodamine has low sensitivity to the dielectric constant of the medium, this increase of fluorescence is very likely related to the dissociation of aggregated DS3 or DS4 in the presence of lipid vesicles. Due to the difference in their aggregation state, the initial levels of fluorescence of Rho-labeled DS3 and DS4 were not identical. Nevertheless, their fluorescence came almost to an equal level after the addition of lipid vesicles. Moreover, the kinetics of dissociation (Fig. 5*B*) reflects that DS4 dissociates much slower than DS3, indicating that the packing of DS4 aggregates is tighter than DS3 aggregates. The monomeric existence of DS3 and DS4 in their membrane-bound state was further confirmed by energy transfer experiments, where the observed energy transfers between NBD-DS3/Rho-DS3 or NBD-DS4/Rho-DS4 either in PC or PS/PC vesicles were similar to those of randomly distributed monomers (data not shown).

DISCUSSION

The mechanism by which most antimicrobial peptides known to date exert their cytotoxic activity is not clearly understood. Accumulating data, however, suggest that peptide-membrane interaction is a primary step for their functioning and that the charge and the hydrophobic properties of the peptide are of importance. In this respect, members of the broad spectrum antimicrobial peptides dermaseptins appeared as ideal tools to assess the implication of such parameters. These water-soluble peptides, which are predicted to form amphipathic α-helices, interact with biological membranes and exhibit selective properties toward membranes of varied phospholipid compositions (6, 14). Among the dermaseptins, DS3 and DS4 are of particular interest, since the polar surface of the helix is of the same size (forming an angle of 110° in both peptides). DS4, however, is significantly more hydrophobic than DS3 (hydropathic index +28.9 and +10.5, respectively (15)). Moreover, while the four positive charges of DS4 are concentrated in the middle, the five net positives charges of DS3 are regularly spaced along the helix. The present study aimed at characterizing a possible influence of these parameters on peptide-peptide and peptide-membrane interactions. The fluorescence dequenching experiments using Rho-DS3 and Rho-DS4 demonstrated that both peptides are aggregated in aqueous solution. However, the aggregational state of DS4 is higher than that of DS3. Both peptides interacted with the plasma membrane of erythrocytes, and binding resulted in cell permeation. Yet, whereas low concentrations of DS4 permeated the cells, DS3 bound to the red cells at low concentrations without causing apparent cell damage and cell permeabilization occurred only when a critical concentration was achieved. We speculate, in light of these observations, that the higher aggregation of DS4 in solution allows reaching, upon contact with the cell, a local (at the impact point) effective concentration for cell permeation. Likewise, the aggregation state of the peptide in solution may also influence both the spectrum of antimicrobial activity and the mechanism of action. In a previous study, DS4 was found generally less active than DS3 (15) in killing microorganisms such as the Gram-negative bacterium *E. coli*. Such organisms are endowed with external membranes that prohibit direct interaction of the peptide with the microbial plasma membrane. The antibacterial effect observed in that case probably results from destabilization of the external membranes, a process in which less aggregated DS3 seems more efficient. The fact that dermaseptin S1, which is not aggregated in aqueous solution, was more active than either DS3 or DS4 against *E. coli*, supported this notion. On the other hand, in microorganisms that allow access to plasma membrane, such as protozoan parasites *Leishmania* sp., DS4 was clearly more potent than DS3 in inducing instant cell lysis,[2] much as observed with erythrocytes.

The N-terminal ends of both DS3 and DS4 are buried slightly inside the hydrophobic core of either zwitterionic PC or negatively charged PS/PC lipid vesicles. This was revealed by the experiments with NBD-labeled peptides, where insertion of the N-terminal ends of the peptides caused a blue shift of NBD emission maxima around 527 nm. Such NBD emission maxima correspond to a more hydrophobic environment than the hydrophilic surface, which exhibits NBD emission maximum of 533 nm, and is less hydrophobic than the bilayer core, which is characterized by an NBD emission maximum of 522 nm (33). Proteolytic cleavage experiments also supported this notion. Since the N-terminal ends of DS3 and DS4 were buried within the hydrophobic core of the zwitterionic or negatively charged lipid bilayer, proteinase K treatment of the membrane-bound NBD-labeled peptides did not induce a change in NBD fluorescence. This suggested that the peptides are oriented in a way that their hydrophobic face is embedded relatively shallowly within the hydrophobic region of the membrane and their positive charges directed toward the hydrophilic region. In such orientation, DS3 and DS4 would be protected from the proteolytic cleavage. For comparison, in similar experiments performed with dermaseptin S1, the peptide was found to be susceptible to proteolytic treatment when bound to PC but not to PS/PC vesicles (6). The high susceptibility of dermaseptin S1 to proteolytic digestion when bound to zwitterionic vesicles suggests a more superficial interaction.

Interestingly, aggregated DS3 and DS4 dissociate into monomers upon interaction with either PS/PC or PC vesicles. This is evidenced in Fig. 5*B* and further supported by energy transfer experiments using NBD-labeled donor/Rho-labeled acceptor of DS3 and DS4. The monomeric state of DS3 and DS4 in the lipid bilayer is contrasted with the aggregational state of channel-forming peptides, such as alamethicin, pardaxin, and helix 2 of Bti δ-endotoxin (3–5, 16, 36). This rules out the possibility that a "barrel stave" mechanism is the mode of action of DS3 and DS4. This mechanism involves three distinct steps. First, monomers bind to the membrane; second, these monomers insert into the lipid bilayer; and finally, the monomers aggregate into a barrel-like structure with a central aqueous pore surrounded by peptide or protein. Here, we propose that a nonpore carpet-like mechanism is involved in the membrane permeating activity of DS3 and DS4, as was suggested for the antimicrobial peptides cecropins, magainins, and dermaseptins

[2] J. K. Ghosh, D. Shaool, P. Guillaud, L. Cicéron, D. Mazier, I. Kustanovich, Y. Shai, and A. Mor, unpublished results.

S1 or B1 (6, 7, 14, 37–39). In this mechanism, four steps were postulated to be involved: (i) preferential binding of peptide monomers to the phospholipid vesicles, (ii) laying of amphipathic α-helical monomers on the surface of the membranes so that the positive charges of the basic amino acids interact with the negatively charged phospholipid head groups or with water molecules, (iii) rotation of the molecule leading to reorientation of the hydrophobic residues toward the hydrophobic core of the membrane, and (iv) disintegrating the membrane by disrupting the lipid packing in the bilayer structure (35).

DS3 and DS4 were found to be highly potent in their ability to dissipate diffusion potentials in both PC and PS/PC vesicles. This observation is different from what was reported with the nonhemolytic antibacterial peptides. Dermaseptins S1 and B1 (6, 14), cecropins P and B, magainins, and diasteromers of the cytolytic peptides pardaxin (40, 41) were shown to selectively permeate PS/PC but not PC vesicles. We speculate that the phospholipid charge difference, which represents one among many parameters responsible for selective permeabilization by these peptides, is overwhelmed by yet another parameter: the organization of the peptides in solution prior to contact with the membrane. Since DS3 and DS4 bind to the phospholipid membrane initially as aggregated molecules, large numbers of molecules are accumulated at the target point in a shorter time compared with those that originally bind to the membrane as monomers. Moreover, permeation of the PS/PC bilayer was similar between DS3 and DS4 in terms of potency and kinetics, but DS4 was more potent in PC vesicles and acted with faster kinetics. We propose that there are two major differences between DS3 and DS4 that might be responsible for the higher membrane permeabilization activity of DS4. First, DS4 is in higher aggregational state and takes longer time to dissociate in the membrane. Second, the absence of charged residues at the extremities of DS4 may facilitate stronger hydrophobic interaction with the acyl chains in zwitterionic PC bilayer. In this respect, since the major component in erythrocyte membrane outer leaflet is PC (42, 43), the higher efficiency of DS4 in perturbing the packing order of PC vesicles may be related to its higher hemolytic activity.

Finally, in concordance with previous findings concerning other dermaseptin members, the present study provided firm evidence that DS3 and DS4 are also highly lipophilic peptides that spontaneously partition into the lipid phase. Therefore, thermodynamic considerations argue against the likelihood that once bound to plasma membrane, dermaseptins would spontaneously translocate and reach an intracellular target. The exclusively peripheral localization of Rho-DS3 and Rho-DS4 in noninfected erythrocytes (Fig. 1) indeed indicated that the peptides do not translocate across the plasma membrane but integrate/associate in a stable manner within the lipid bilayer. In infected cells, however, the peptides seemed to interact directly with the parasite (Fig. 3). Moreover, both DS3 and DS4 were able to affect the viability of the intraerythrocytic parasites at concentrations that did not permeate the host cell (Fig. 4). At present, it is not clear how dermaseptins reached the intracellular location. The question of how intraerythrocytic parasites obtain exogenous nutrients and specifically, macromolecules, is controversial (44–49), and its resolution lies out of the scope of the present investigation. The fact that is relevant to the antimalarial effect of dermaseptins is their demonstrable ability to enter into infected RBC and kill the parasite.

Acknowledgments—We are thankful to Prof. Rachel Nechushtai (The Hebrew University of Jerusalem) for critical reading of the manuscript.

REFERENCES

1. Boman, H. G. (1995) *Annu. Rev. Immunol.* **13,** 61–92
2. Nicolas, P., and Mor, A. (1995) *Annu. Rev. Microbiol.* **4,** 277–304
3. Fox, R. O., and Richards, F. M. (1982) *Nature* **300,** 325–330
4. Schwarz, G., Gerke, H., Rizzo, V., and Stankowski, S. (1987) *Biophys. J.* **52,** 685–692
5. Shai, Y. (1994) *Toxicology* **87,** 109–129
6. Pouny, Y., Rapaport, D., Mor, A., Nicolas, P., and Shai, Y. (1992) *Biochemistry* **31,** 12416–12423
7. Bechinger, B., Zasloff, M., and Opella, S. J. (1992) *Biophys. J.* **62,** 12–14
8. Shai, Y. (1995) *Trends Biochem. Sci.* **20,** 460–464
9. Mor, A., Nguyen, V. H., Delfour, A., Migliore-Samour, D., and Nicolas, P. (1991) *Biochemistry* **30,** 8824–8830
10. Mor, A., and Nicolas, P. (1994) *Eur. J. Biochem.* **219,** 145–154
11. Mor, A., Amiche, M., and Nicolas, P. (1994) *Biochemistry* **33,** 6642–6650
12. Mor, A., and Nicolas, P. (1994) *J. Biol. Chem.* **269,** 1934–1939
13. Hernandez, C., Mor, A., Dagger, F., Nicolas, P., Hernandez, A., Benedetti, E. L., and Dunia, I. (1992) *Eur. J. Cell Biol.* **59,** 414–424
14. Strahilevitz, J., Mor, A., Nicolas, P., and Shai, Y. (1994) *Biochemistry* **33,** 10951–10960
15. Mor, A., Hani, K., and Nicolas, P. (1994) *J. Biol. Chem.* **269,** 31635–31641
16. Rapaport, D., and Shai, Y. (1992) *J. Biol. Chem.* **267,** 6502–6509
17. Shai, Y., Bach, D., and Yanovsky, A. (1990) *J. Biol. Chem.* **265,** 20202–20209
18. Shai, Y., Hadari, Y. R., and Finkels, A. (1991) *J. Biol. Chem.* **266,** 22346–22354
19. Bartlett, G. R. (1959) *J. Biol. Chem.* **234,** 466–468
20. Papahadjopoulos, D., and Miller, N. (1967) *Biochim. Biophys. Acta.* **135,** 624–638
21. Sims, P. J., Waggoner, A. S., Wang, C. H., and Hoffmann, J. R. (1974) *Biochemistry* **13,** 3315–3330
22. Loew, L. M., Rosenberg, I., Bridge, M., and Gitler, C. (1983) *Biochemistry* **22,** 837–844
23. Desjardin, R. E., Canfield, C.j., Haines, J. D., and Chulay, J. D. (1979) *Antimicrob. Agents Chemother.* **16,** 710–718
24. Trager, W., and Jensen, J. B. (1976) *Science* **193,** 673–675
25. Mirovski, P., Gay, F., Bustos, D., Mazier, D., and Gentilini, M. (1990) *Trans. R. Soc. Trop. Med. Hygiene* **84,** 511–515
26. Wuthrich, K. (1986) *NMR of Proteins and Nucleic Acids*, John Wiley & Sons, Inc., New York
27. Kenner, R. A., and Aboderin, A. A. (1971) *Biochemistry* **10,** 4433–4440
28. Frey, S., and Tamm, L. K. (1990) *Biochem. J.* **272,** 713–719
29. Gazit, E., and Shai, Y. (1993) *Biochemistry* **32,** 3429–3436
30. Gazit, E., and Shai, Y. (1993) *Biochemistry* **32,** 12363–12371
31. Mao, D., and Wallace, B. A. (1984) *Biochemistry* **23,** 2667–2673
32. Rajarathnam, K., Hochman, J., Schindler, M., and Ferguson, M. S. (1989) *Biochemistry* **28,** 3168–3176
33. Chattopadhyay, A., and London, E. (1987) *Biochemistry* **26,** 39–45
34. Gazit, E., Lee, W.-J., Brey, P. T., and Shai, Y. (1994) *Biochemistry* **33,** 10681–10692
35. Gazit, E., Boman, A., Boman, H. G., and Shai, Y. (1995) *Biochemistry* **34,** 11479–11488
36. Schwarz, G., Stankowski, S., and Rizzo, V. (1986) *Biochim. Biophys. Acta* **861,** 141–151
37. Matsuzaki, K., Harada, M., Funakoshi, S., Fujii, N., and Miyajima, K. (1991) *Biochim. Biophys. Acta* **1063,** 162–170
38. Bechinger, B., Zasloff, M., and Opella, S. J. (1993) *Protein Sci.* **2,** 2077–2084
39. Matsuzaki, K., Murase, O., Tokuda, H., Funakoshi, S., Fujii, N., and Miyajima, K. (1994) *Biochemistry* **33,** 3342–3349
40. Oren, Z., and Shai, Y. (1996) *Eur. J. Biochem.* **237,** 303–310
41. Oren, Z., and Shai, Y. (1997) *Biochemistry* **36,** 1826–1835
42. Verkleij, A. J., Zwaal, R. F., Roelofsen, B., Comfurius, P., Kastelijn, D., and Deenen, L. V. (1973) *Biochim. Biophys. Acta* **323,** 178–193
43. Op den Kamp, J. A. F., Roelofsen, B., and Van Deenen, L. L. M. (1985) *Trends Biochem. Sci.* **10,** 320–323
44. Haldar, K. (1994) *Parasitol. Today* **10,** 393–395
45. Gero, A. M., and Kirk, K. (1994) *Parasitol. Today* **10,** 395–399
46. Taraschi, T. F., and Nicolas, E. (1994) *Parasitol. Today* **10,** 399–401
47. Hibbs, R. A., Stenzel, D. J., and Saul, A. (1996) *Eur. J. Cell Biol.* **72,** 182–188
48. Pouvelle, B., Spigel, R., Hsiao, L., Howard, R. J., Morris, R. L., Thomas, A. P., and Taraschi, T. F. (1991) *Nature* **353,** 73–75
49. Grellier, P., Rigomier, D., Clavey, V., Fruchart, J. C., and Schrevel, J. (1991) *J. Cell Biol.* **112,** 267–277